



# Polydopamine coating of living diatom microalgae

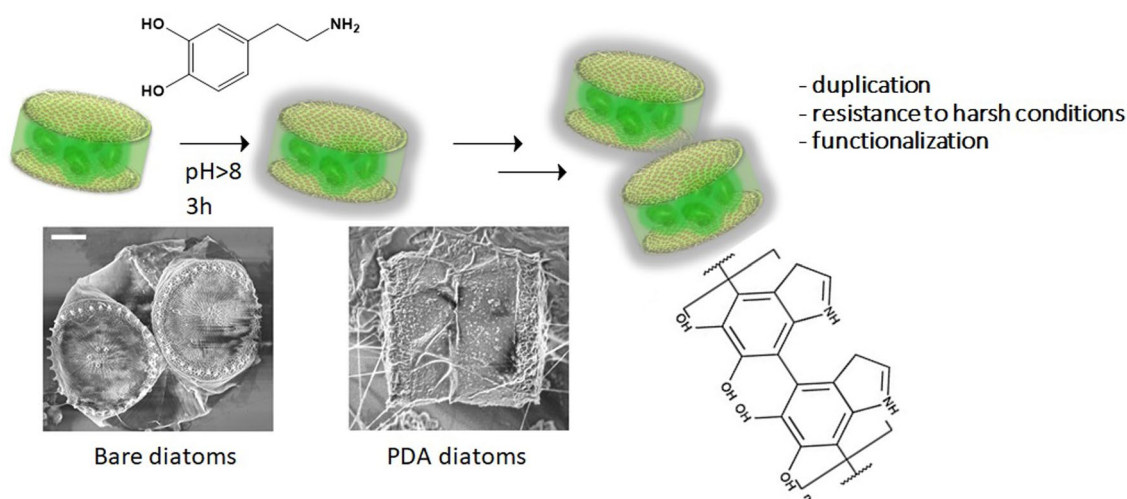
Danilo Vona<sup>1</sup> · Stefania R. Cicco<sup>2</sup> · Roberta Ragni<sup>1</sup> · Cesar Vicente-Garcia<sup>1</sup> · Gabriella Leone<sup>1</sup> · Maria Michela Giangregorio<sup>3</sup> · Fabio Palumbo<sup>3</sup> · Emiliano Altamura<sup>1</sup> · Gianluca M. Farinola<sup>1</sup>

Received: 10 December 2021 / Accepted: 31 January 2022  
© The Author(s) 2022

## Abstract

Many microorganisms produce specific structures, known as spores or cysts, to increase their resistance to adverse environmental conditions. Scientists have started to produce biomimetic materials inspired by these natural membranes, especially for industrial and biomedical applications. Here, we present biological data on the biocompatibility of a polydopamine-based artificial coating for diatom cells. In this work, living *Thalassiosira weissflogii* diatom cells are coated on their surface with a polydopamine layer mimicking mussel adhesive protein. Polydopamine does not affect diatoms growth kinetics, it enhances their resistance to degradation by treatment with detergents and acids, and it decreases the uptake of model staining emitters. These outcomes pave the way for the use of living diatom cells bearing polymer coatings for sensors based on living cells, resistant to artificial microenvironments, or acting as living devices for cells interface study.

## Graphical abstract



**Keywords** Diatoms · Biopolymers · Polydopamine · Artificial coating · Chloroplasts

✉ Danilo Vona  
danilo.vona@uniba.it

- <sup>1</sup> Department of Chemistry, Università degli Studi “Aldo Moro”, Via Orabona 4, 70126 Bari, Italy
- <sup>2</sup> Department of Chemistry, CNR-ICCOM-Bari, Via Orabona 4, 70126 Bari, Italy
- <sup>3</sup> Institute of Nanotechnology, CNR-NANOTEC, c/o Dipartimento di Chimica, Università di Bari, via Orabona 4, 70126 Bari, Italy

## 1 Introduction

Over the last decades several scientific works have been focused on the study of synthetic materials tailored to control interaction of cells with extracellular matrices, and to increase cell stability [1]. Organic chemistry and polymer science play a crucial role for this aim. Living cells can be directly functionalized and proposed as an efficient

alternative to the artificial materials for a variety of applications, including sensing and catalysis. Single cell modification is a fascinating tool based on the introduction of non-biogenic functional groups [2], macromolecular structures on the cell surface [3], or inside the cytoplasm. Some of these chemical modifications consist on the production of artificial thin coatings to increase living cells resistance to harsh conditions [4]. In Nature, bacteria, fungi, microalgae and upper plants have evolved several mechanisms to preserve themselves under unfavourable external conditions. In particular, the survival of some marine organisms relies on endowing themselves with shells and spores which protect their genetic information by cellular encapsulation mechanisms [5]. These structures commonly exhibit robustness and resistance, and they increase the cell stability without altering cell–cell or cell–matrix interactions. Once coated, living cells should work together with biotic elements to firmly maintain an ecological equilibrium, by colonizing the surrounding environment while responding to external events.[6]. Among the biomimetic materials, spore-like coatings based on inorganic materials, such as silica [7], and calcium carbonate, have been first proposed to coat yeasts cells [8], as well as titania to coat single *Chlorella* microalgae cells [9]. Nevertheless, these structures exhibited rigidity interfering with cells duplication. Hence, polyelectrolyte multilayers have been investigated as alternative artificial coatings for cells, being are softer and more adaptable to deformation than inorganic coatings [4]. Examples of polyelectrolyte-based systems explored so far are poly(amines) and poly(styrene sulfonate) for yeast cells coatings [10], poly(lysine) and poly(glutamic acid) for *Bacillus subtilis* bacteria cells [11], poly(dimethyldiallyl ammonium chloride) and poly(styrene sulfonate) for human pancreatic islets [12]. A multilayer coating made of chitosan, alginate, hyaluronic acid and oligonucleotide polyelectrolytes was also proposed for *E. coli* both to increase cells resistance and promote oligonucleotide delivery for gene therapy [13]. Polyelectrolyte coating is limited to electrostatic layer-by-layer (LbL) self-assembly of polyanions and cations, allowing resistance to low pH values and salinities over 3%.

Polydopamine (PDA) was very recently used as coating layer for *Saccharomyces cerevisiae* yeast cells to increase their resistance against external agents (such as lytic enzymes), without interfering with cell division and allowing further functionalization of yeast cells with biomolecules for biotechnological applications [14]. However, yeasts are not the sole organisms that can benefit from PDA properties. A PDA homogeneous layer was also used to shelter antigenic epitopes on red blood cells (RBCs): it did not exhibit negative effects on red cell structure and function, especially on oxygen transport [15]. Moreover, PDA was employed to coat single rod-like tobacco mosaic virus (TMV) particles assembled in nano-fibers and covered with gold nanoparticles [16].

Polydopamine is a mussel-bioinspired material produced via oxidative polymerization of dopamine (DA), a biological catecholamine neurotransmitter being also the main component of mussel adhesive proteins [17]. DA is easily polymerizable under alkaline conditions [18], and the polydopamine coating is soft, adhesive [19], biocompatible and suitable for further chemical functionalization [20]. PDA represents a versatile coating polymer in several fields of applications ranging from tissue engineering [21], to organic electronics [22]. In this paper, we investigate the *in vivo* PDA encapsulation of single *Thalassiosira (Conticribra) weissflogii* diatom cells to explore for the first time the effects of PDA on diatoms' viability. Diatom microalgae represent an amazing example of encased biological structures and they are natural sources of mesoporous silica useful for photonics and biomedicine [23]. Diatom frustules exhibit a hierarchically organized nanostructured architecture of silica layers with different porosity, high surface area and tunability of pore size depending on the algal species. Moreover, a great advantage consists in the possibility to functionalize both *in vivo* [24], and *in vitro* [25], diatoms' biosilica for biomedical, photonic [26], optoelectronic and photobiological applications [27, 28]. We demonstrate here that the encapsulation of single diatom cells in PDA has a very limited impact on the viability of the cells, and it is an efficient protocol to increase cell resistance to harsh environmental conditions, paving the way to the possibility of using highly resistant living diatoms for potentially manifold technological applications.

## 2 Results

In this work, living *Thalassiosira weissflogii* single cells have been encapsulated with a protective organic PDA shell. A direct *in situ* oxidative DA polymerization was carried out in the algal culture under weak alkaline conditions (pH 8.2), according to the protocol reported in the Experimental Section. As first attempt, five different DA concentrations (0, 0.25, 0.75, 2, 3, 5 mg/mL) have been tested and then cells have been checked using reflection microscopy after sampling and deposition over reflecting silicon surfaces. Reflection microscopy images (Fig. 1a) revealed a generalized blackening of the cells, as an effect of PDA coating formation, which increased overtime. PDA was found also inside the box-like structures which kept their integrity and individual shapes. Debris of cells and external PDA aggregates were particularly abundant at 5 mg/mL DA concentration. Once the coatings were obtained, cell growth kinetics were performed for each DA concentration using fresh diatoms medium and starting from the same cell density ( $5 \times 10^4$  cells/mL; Fig. 1b). A normal growth trend was observed for 0.25 mg/mL of dopamine and an increase in lag phase time

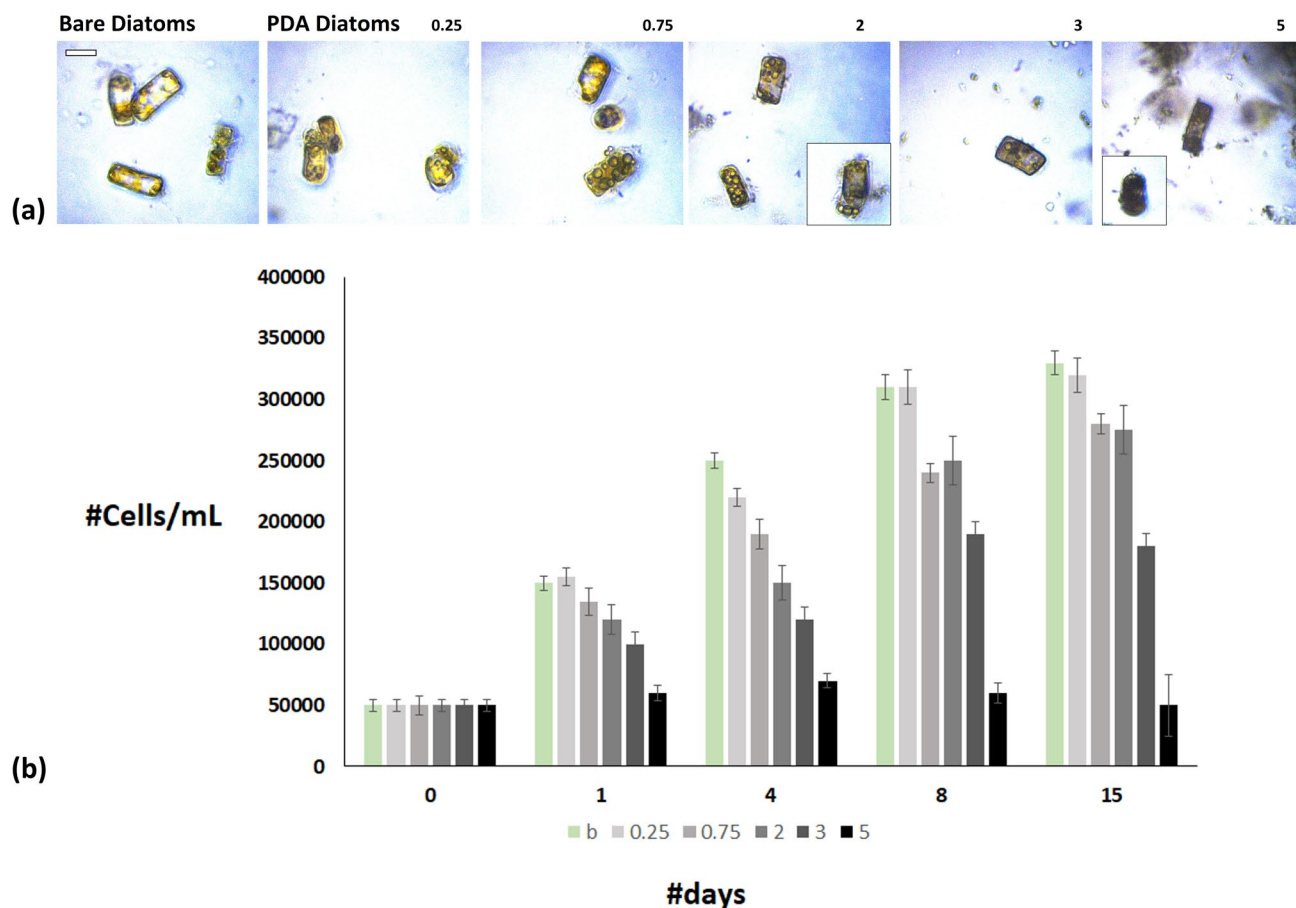


**Fig. 1** **a** Reflection microscopy pictures of living bare and PDA-coated microalgae starting from different dopamine concentrations. Scale bar: 5  $\mu$ m. **b** Cell kinetics histograms of bare and coated living microalgae over 1, 4, 8 and 15 days of culture

was found for 0.75 and 2 mg/mL, although reaching a final biomass of 75% over the control biomass. Finally, polydopamine obtained from the highest concentrations resulted detrimental also in terms of biomass at semi-plateau.

Living *Thalassiosira weissflogii* diatoms were then subjected to both single and double coating treatments, using a dopamine concentration of 2 mg/mL, to evaluate the effect of the PDA layer thickness on cells growth kinetics. Reflection microscopy images (Fig. 2a) show that, after a single coating treatment, diatoms appear as brownish microalgae and retain their individual shape, whereas double coating induces the formation of stacked cells with external clusters or PDA aggregates outside cells. Cell growth kinetics (Fig. 2b) was not affected by the single PDA coating although a prolonged lag phase was observed likely due to cells quiescent state [14], whereas a growth rate reduction was recorded for the double-PDA-coated cells.

Since PDA double layer strongly inhibited diatom growth, we focused attention on the investigation of the single PDA coating as an efficient method of single-cell encapsulation, mainly, as protective coating, without altering cell division.

A UV-Vis absorption spectrum (Fig. 3) was recorded for PDA-coated diatoms (PDA@diatoms) and compared with those of PDA nanoparticles (Fig. 3a, See “Methods”), the DA monomer and non-coated diatoms. The PDA@diatoms spectrum showed a broad band centered at 300 nm which confirmed the presence of PDA around the cell, overlapping the spectral region of diatoms’ biosilica scattering [29–31]. Moreover, the absorption peaks of Chlorophyll *a* and *c* centered at 450 nm and 685 nm are evident in the spectrum of untreated cells are hidden by PDA absorption scattering signal. The FT-ATR spectra for the PDA nanoparticles, the bare *Thalassiosira weissflogii* diatom cells (Bare Diatoms) and polydopamine-coated diatoms (PDA Diatoms) are shown in Fig. 3c. The spectra of coated diatoms contain multiple and complex signals around 1440, 1610 and 1720  $\text{cm}^{-1}$ , corresponding to the stretching modes for the indole, C=C quinone and carbonyl moieties related to the PDA backbone. Moreover, the stretching signal of water around 3455  $\text{cm}^{-1}$  exhibits a shoulder signal around 3260  $\text{cm}^{-1}$  corresponding to internal amine-based moieties [30].

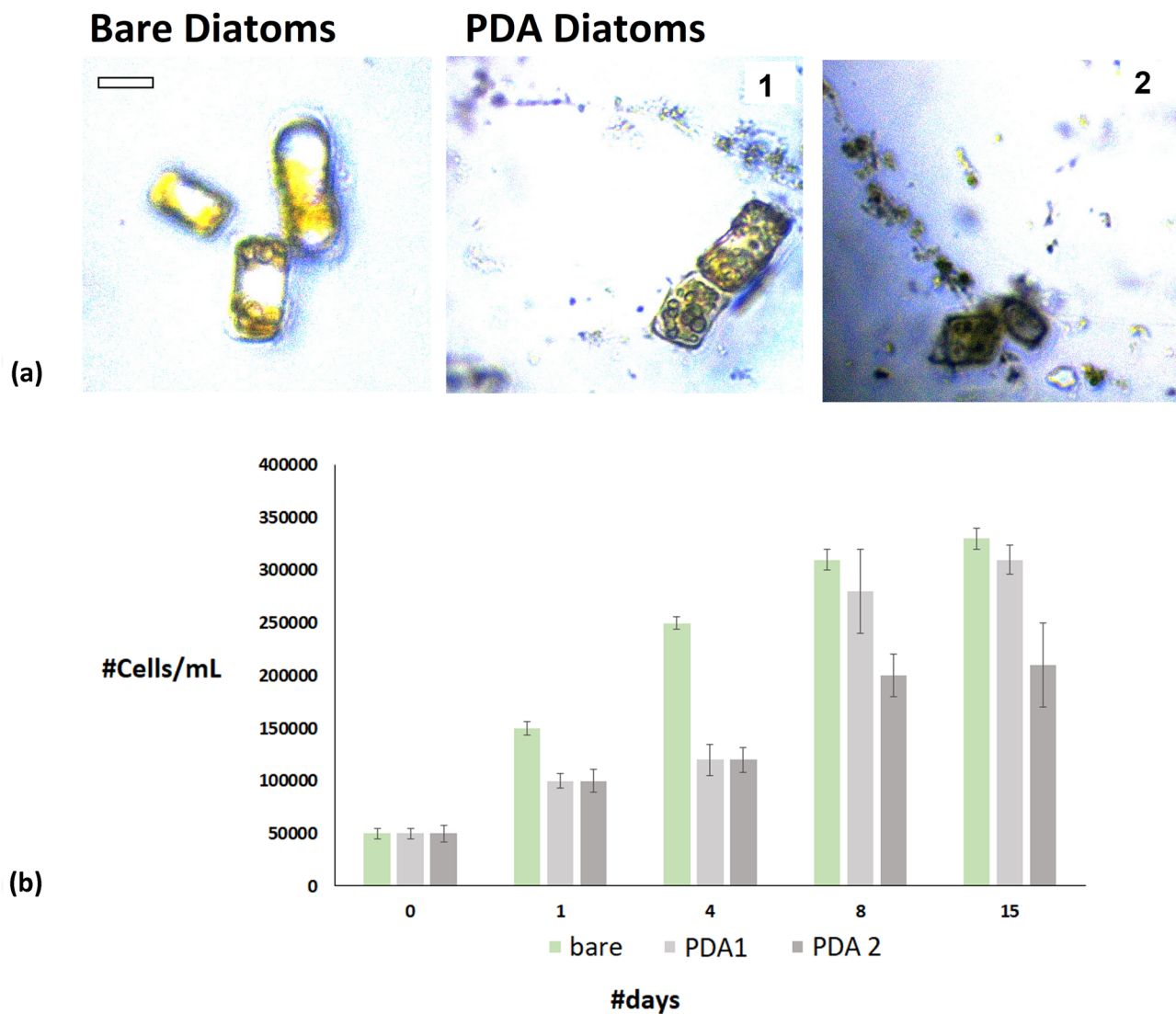


**Fig. 2** **a** Reflection microscopy pictures of living bare, single PDA (PDA1) and double PDA (PDA2)-coated *Thalassiosira weissflogii* diatoms. Scale bar: 10  $\mu$ m. **b** Cell kinetics histograms of bare, single-PDA and double-PDA-coated diatoms over 1, 4, 8 and 15 days of culture

PDA-coated and bare diatoms were then spotted on silicon for SEM characterization and on glass for AFM investigation (Fig. 4). Interestingly, the PDA layer seems to effectively protect the integrity of the diatom micro-shells, that are usually dramatically compressed during the process of vacuum-assisted dehydration (Fig. 4a). This process has been statistically validated for 81% of the observed fields (25). SEM and AFM images in Fig. 4 reveal that after the PDA coating, both PDA layer and nanoparticles appear on the silica structures. Topographical data and the corresponding “error signal” images clearly show an increase in the surface granularity of the PDA-coated diatoms, more specifically, with an increase in the surface roughness from 470 nm (for the bare diatom) to 540 nm. PDA particles have a diameter in the range of  $350 \pm 80$  nm, and reach an average

thickness (height) in the range  $160 \pm 50$  nm. Similarly, for the bare diatoms the phase image is homogeneous in comparison with the one from PDA-coated diatoms. The latter exhibit different chemical phase contrast due to the PDA particles. Both SEM and AFM images show that the PDA distribution and coverage on the silica structure is quite uniform.

After the morphological characterization of the PDA-coated cells, biological parameters such as cell viability, permeability and chemical resistance were also studied. Morphology and cell behaviour of PDA-coated diatoms were investigated by confocal microscopy. Confocal microscopy analysis (Fig. 5a) and 3D merge reconstruction (Fig. 5b) performed on bare and PDA diatoms show the presence of a dark layer around the cell after the polymerization process: the chemical decoration occurs not only

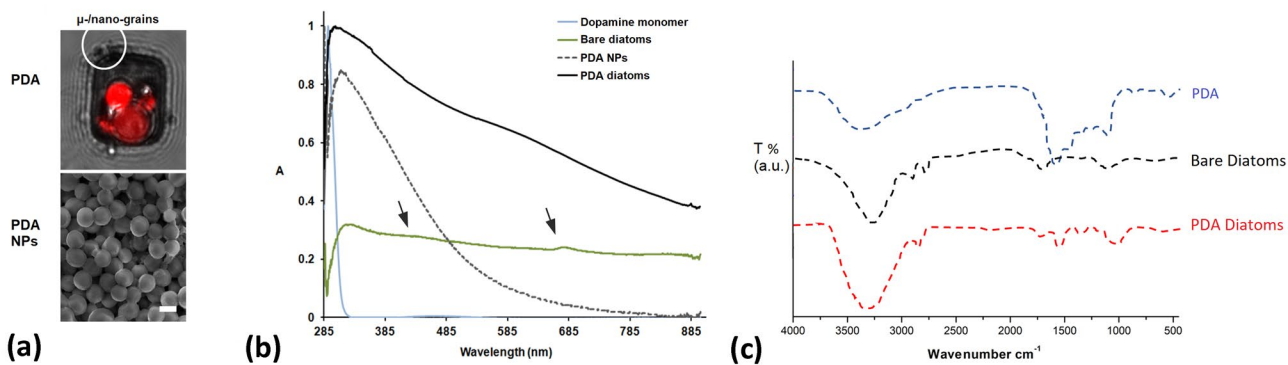


**Fig. 3** **a** Confocal microscopy image of a single PDA-coated diatom and a SEM image of PDA nanoparticles (PDA NPs; marker: 200 nm) used as a control sample for the UV-characterization. **b** UV-visible adsorption spectra of dopamine monomer, bare diatoms, PDA nano-

particles and PDA-coated living cells in distilled water. **c** FT-ATR spectra comparison of lone PDA, bare diatom cells (Bare Diatoms) and PDA-coated diatoms (PDA Diatoms)

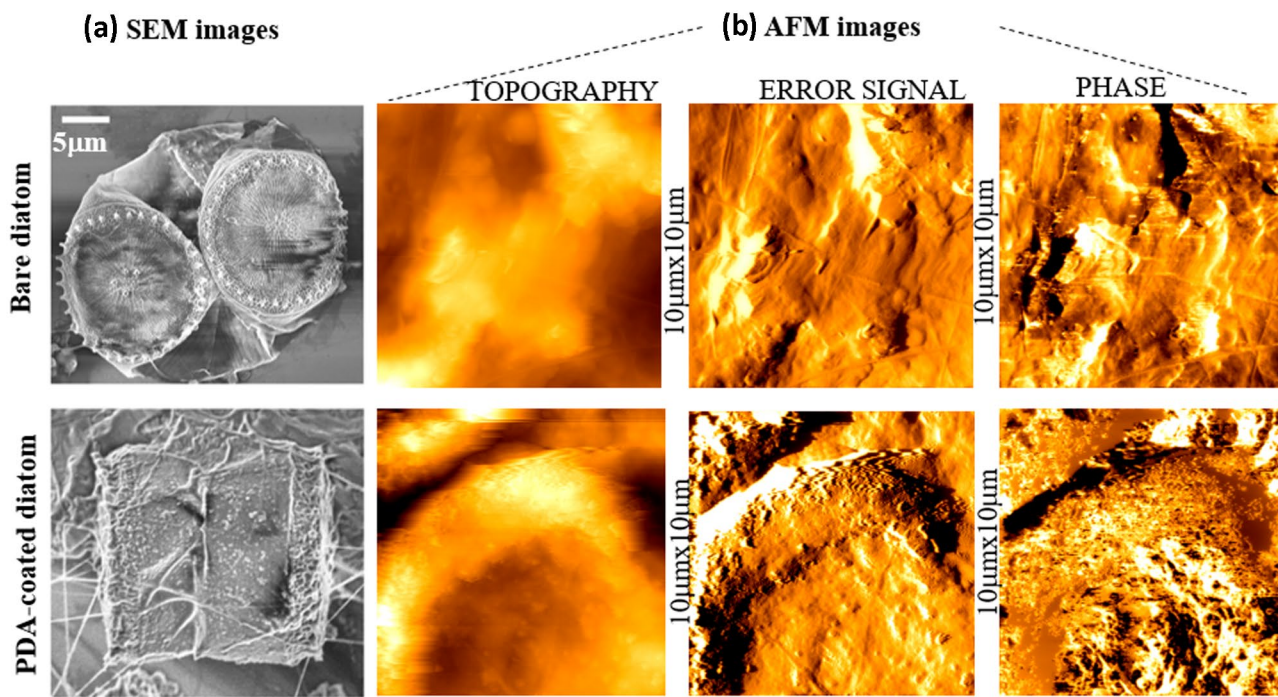


**Fig. 4** **a** Scanning electron microscopy (SEM) pictures **a**, **b** 10 μm × 10 μm Atomic force microscopy (AFM) images of bare and PDA-coated diatom cells

on the box-like shells, but also inside sub-cell structures. Inside cells, chloroplast mottles are still red emissive, compartmentalized and polarized: these data, together with a fine cell morphology, constitute strong evidence of maintained diatoms viability, even if the presence of the PDA coating [32]. 3D comparison analysis allowed us to determine that a PDA capsule ( $1.17 \pm 0.388 \mu\text{m}$  in thickness) is formed all over the whole transparent shell of *Thalassiosira weissflogii* after functionalization.

Moreover, PDA-coated diatoms retain their ability to produce mitotic biological sub-structures. In details, elongated, connective, mitotic sub-structures are visible in PDA-coated cells using a sodium metasilicate surplus to enhance cell duplication (Fig. 5c, di). As shown in confocal micrograph focus (Fig. 5di–diii), PDA layer surrounds the whole diatom structure preserving its box-like shape, without altering chloroplasts that appear still red emissive, compartmentalized, and polarized along the silica walls.

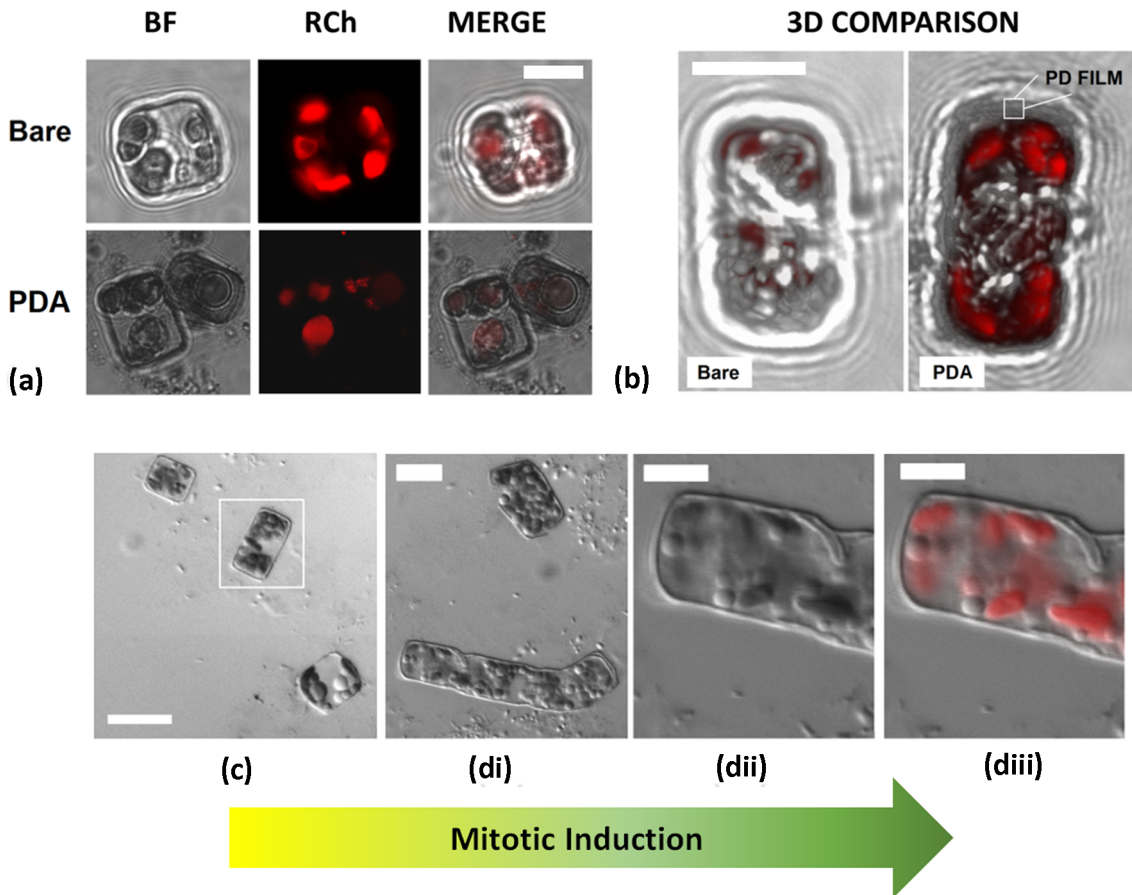


**Fig. 5** Confocal microscopy images of single PDA-coated diatom and bare cells (**a**, scale bar: 5  $\mu$ m), 3D merge reconstruction (**b**, scale bar: 5  $\mu$ m) and morphological behaviour of coated cells before (**c**, scale

bar: 10  $\mu$ m) after sodium metasilicate-induced mitosis (**di**. low magnification, scale bar: 5  $\mu$ m; **dii**. high magnification; **diii**. high magnification merged with chloroplasts emission, scale bar: 2  $\mu$ m)

Cell viability of PDA-coated cells was also checked using flow cytometry output comparison (Fig. 6) with non-coated cells, as reported in the Materials and Instruments section. Bare cells (control sample) were analyzed to set scattering and fluorescence thresholds. The parameter chosen as

discriminator between living and dead cell populations was chloroplast-bearing bright red fluorescence. In particular, red emission of chloroplasts was recorded with a  $670 \pm 15$  nm bandpass filter. An arbitrary red fluorescence value was fixed as the highest value of viability for healthy cells. Diatoms

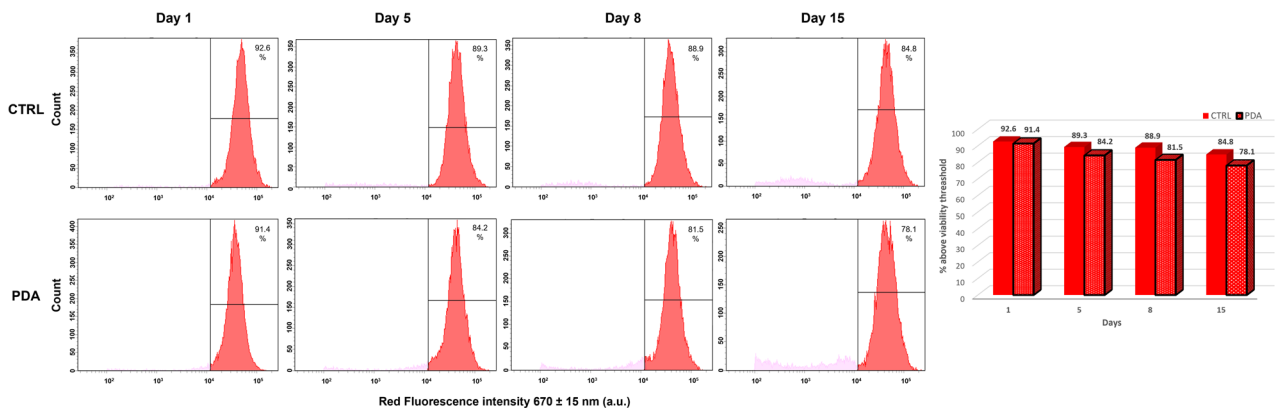


**Fig. 6** Cytometric evolution of bare (ctrl) and PDA-coated diatom cells shown as distributions and bar histograms over times

functionalized with PDA, analyzed in parallel with the control sample after 1, 4, 8 and 15 days of culture, as evidenced in Fig. 6, exhibit positive parameters related to the viability largely above the 60% of the overall cell population. Thus, strongly supporting the positive biocompatibility of PDA polymer coating.

The capacity of the PDA as protective coating for living cells was assessed by exposing coated cells to different harsh environmental conditions. Briefly, the bare and coated diatoms were treated with 10%v/v HCl and 1%v/v sodium dodecyl sulphate (SDS) solution at 55 °C (Fig. 7a, b). Viability tests after the treatment were performed by auto-fluorescence assay, with auto-fluorescence expressed as the ratio of number of cells with red emitting chloroplasts, observed by confocal fluorescence microscopy, over the total number of cells observed in bright field. After addition of the HCl/SDS solution, chloroplasts of PDA-coated living diatoms were found to be still red emitting, integral and viable, as opposed to the bare cells used as the control, that had lost the chloroplast fluorescence. Permeability of the PDA layer on cells surface was also explored (Fig. 7c) performing an incubation of control and coated cells with Rhodamine 123 [33], a dye usually suitable for staining cells cytoplasm. A confocal microscopy investigation was performed at different times of incubation, using fluorescein exc./em. parameters for Rhodamine123 detection, and TRITC exc./em. parameters for chloroplasts luminescence analysis. PDA seems to act as an artificial external membrane which avoids the inclusion of the staining agent inside cells.

To test the capacity of the PDA-coating to sustain further functionalization, we have successfully decorated the PDA layer with silver nanoparticles (Ag-NPs) directly deposited onto the living cells. Thus, taking advantage from adsorptive, chelating and reducing ability

of poly-hydroxy-indole functionalities. Living diatoms coated with PDA and silver were prepared using a standard procedure and characterized by Scanning Electron Microscopy (Fig. 8) and EDX. SEM analyses revealed that the Ag-NPs (d–e) covered about all the living PDA diatom cell (a–c). The size of Ag-NPs produced onto PDA surface was in the range of  $15.38 \text{ nm} \pm 0.9$  (the smaller size) and  $77.1 \text{ } \mu\text{m} \pm 7.4$  (the larger size). Finally, EDX analysis (histograms) was performed to define the atomic element percentage in PDA cells and Ag/PDA cells. The presence of silver on the biohybrids surface was confirmed with values around  $9.825 \pm 1.96\%$ . Silver was absent onto PDA-coated cells.

### 3 Conclusion

Diatom cells have been successfully and individually coated with a layer of polydopamine. The polydopamine guarantees a uniform coverage, and it increases the resistance of these cells to external agents, such as surfactants and strong acid conditions, that are detrimental to cell life. Said resistance enhancement takes place without affecting the natural morphology of the cells, or hampering their ability to undergo mitosis. Further functionalization of the organic polymer is possible, thanks to its inherent chemical diversity, proving its potential as a fundamental tool for general functionalization of living cells, for any further technological application. The synergy that arises from these coated-diatoms being more resilient under harsh conditions, and readily prone to functionalization, paves the ways towards a more general use of these microalgae in long-term industrial processes and applications.

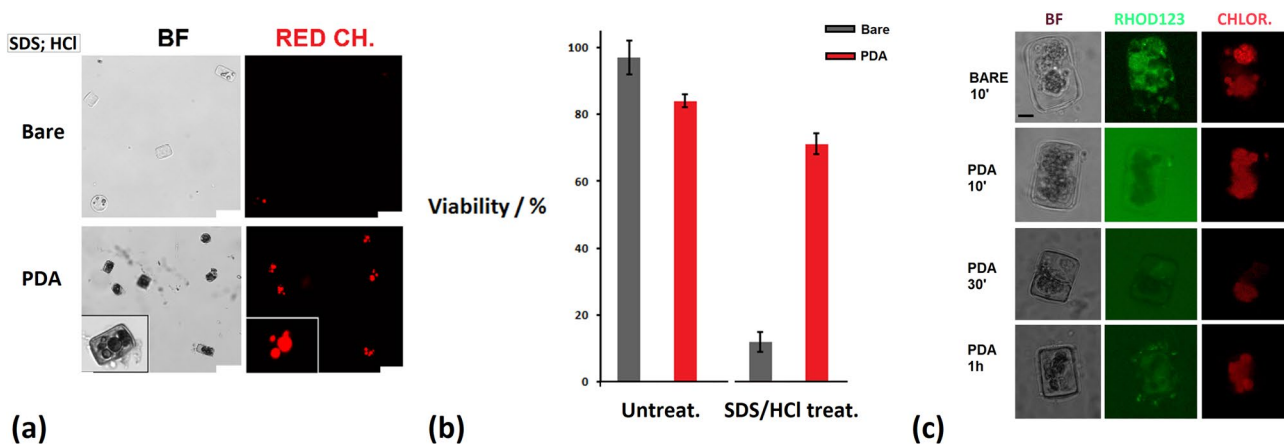


**Fig. 7** **a** Confocal images of bare diatoms (ctrl) and coated (PDA) diatoms after treatment with (HCl/SDS) hot cleaning solutions; **b** histograms of viability % (number of cells with emitting chloroplasts versus number of total cells). **c** Confocal microscopy images of Rhodamine 123 stained diatom cells before (Bare) and after single PDA coating, using bright field, fluorescein and TRITC parameters for Rhod123 and chloroplasts luminescence detection, respectively

damine 123 stained diatom cells before (Bare) and after single PDA coating, using bright field, fluorescein and TRITC parameters for Rhod123 and chloroplasts luminescence detection, respectively

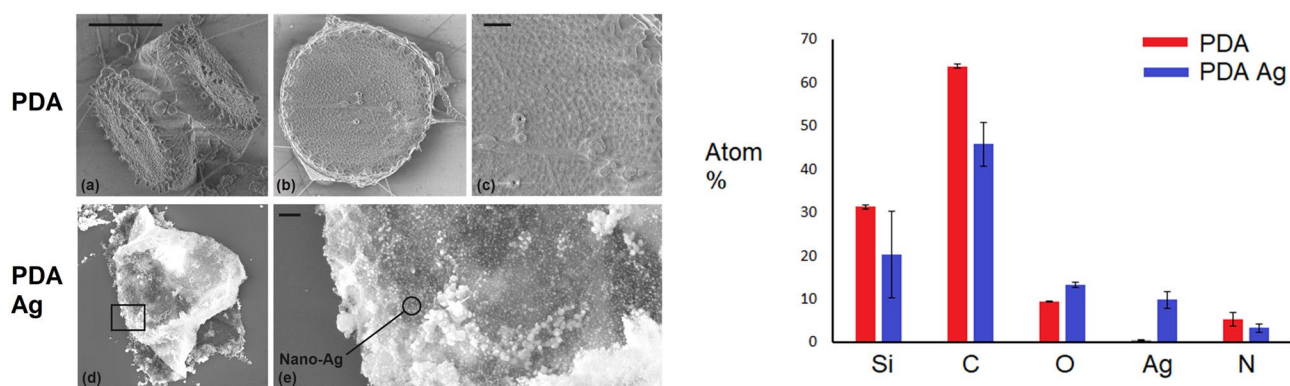


**Fig. 8** SEM images of PDA-coated and PDA Ag-coated living diatoms. Marker: for PDA (a, b, d) 5  $\mu\text{m}$ ; for PDA (c) 1  $\mu\text{m}$ ; for PDA Ag (e), 200 nm. Table: EDX output

## 4 Materials and instruments

Tris(hydroxymethyl)aminomethane hydrochloride, dopamine hydrochloride, potassium hydroxide, rhodamine 123 were purchased from Sigma-Aldrich. *Conticribr* *weissflogii* or *Thalassiosira weissflogii* (culture collection of algae and protozoa, strain 1085/18), F/2 Guillard and sodium metasilicate solution were purchased from CCAP. For AFM characterization, topographic, error and phase data were simultaneously acquired using the AutoProbe CP (Thermo-Microscope) microscope using a gold-coated Si tip with a resonant frequency of 80 kHz in non-contact mode. Light and fluorescent micrographs showed that diatoms when supported on glass assume a crushed shape that is affected by PDA absorption as confirmed by topographical, error and phase images. Scan electron (SE) microscopy equipment consisted of a FEG SEM, Zeiss (3 keV, 0° tilting function) and the confocal microscopy was a Leica SP8 X (bright field function). UV-vis spectra were recorded on a Shimadzu UV-2401 PC spectrophotometer (acquisition parameters: slit width 1 nm; scan sampling 1 nm; single beam mode). Bright-field optical images were recorded in reflection, using Axiomat microscope, Zeiss. Fourier Transformed Infrared-Attenuated Total Reflectance (FTIR-ATR) spectra were acquired with a Perkin Elmer Spectrum Two Spectrophotometer equipped with a 2 × 2 mm diamond crystal. Spectra were recorded in the range 4000–400  $\text{cm}^{-1}$  with a 2  $\text{cm}^{-1}$  resolution, using 0.25  $\text{cm}^{-1}$  acquisition interval and acquiring 32 scans for each sample.

## 5 Methods

### 5.1 Diatom culture conditions

*Conticribr* (*Thalassiosira*) *weissflogii* diatom cells were grown in sterile F/2 Guillard and sodium metasilicate

respectively in suspension and in adhesion on PS flasks (200 mL) in a static batch bioreactor. F/2 Guillard sea water was sterilized in autoclave and filtered twice (0.22  $\mu\text{m}$   $\varnothing$ ). After Guillard stock additions ( $\text{Na}_2\text{SiO}_3 \cdot 9\text{H}_2\text{O}$ , trace metals, and a vitamin mix), the medium was buffered with NaOH (2 N) reaching pH 7.8. Growth was controlled following the standard diatoms parameters ( $T$ : 18  $^\circ\text{C} \pm 2$ , Relative % Humidity: 64%, Light:Dark cycle: 16: 8 h, white light 7000 lx) optimized for obtaining cultures for technological applications [32].

### 5.2 In vivo Polydopamine Encapsulation of Diatoms

Diatom culture (1 mL,  $10^6$  cells/mL) was collected by centrifugation (1250 rpm, 12') and pellet was washed with aqueous NaCl solution (0.85%) and TRIS (tris(hydroxymethyl)aminomethane) buffer (10 mM, pH 8.5). Single PDA coating of diatoms was carried out by adding dopamine hydrochloride (0.25, 0.75, 2, 3, 5 mg) in a suspension of diatom cells in TRIS buffer solution (1 mL; pH 8.2, 10 mM) and gently stirring for 3 h. Several washing steps with the TRIS buffer were performed after the coating treatment. The polymerization of dopamine around cells was confirmed by contrast phase and reflection microscopies and UV-Vis spectroscopy. The double coating treatment was carried out by repeating the procedure of PDA polymerization on single PDA coated diatoms.

### 5.3 PDA nanoparticles synthesis

PDA nanoparticles were prepared dissolving dopamine hydrochloride 1.0 mg in 2 mL of Tris-HCl buffer (10 mM, pH 8.5). The mixture was stirred at room temperature for 5 h under atmospheric oxygen exposure to allow dopamine polymerization. PDA nanoparticles were isolated as pellets by centrifugation at 5000 ×  $g$  for 10 min and resuspended in Tris-HCl buffer.



## 5.4 Flow cytometry

Cell viability of PDA-coated cells was also checked using a BD LSR Fortessa X-20 (Becton, Dickinson and Company, Franklin Lakes, NJ, USA) cell analyzer. The quartz cuvette flow cell in this apparatus is gel-coupled by refractive index-matching optical gel to the fluorescence objective lens (1.2 NA) for optimal collection efficiency. Light emitted from the cuvette was delivered by fiber optics to the detector arrays. For each measurement,  $10^4$  data events were collected using a flow rate of  $12 \mu\text{L min}^{-1}$ . Bare cells (control sample) were analyzed to set scattering and fluorescence thresholds as the parameters that define a living cell population exhibiting bright red fluorescence due to the chloroplasts.

In particular, red emission of chloroplasts was recorded exciting the sample with a 405 nm laser (laser power 50 mW) and the emission was detected through a  $670 \pm 15$  nm bandpass filter.

## 5.5 Cell resistance test

The protection efficiency of single and double PDA layers for cells was tested treating coated and control diatoms with 10%v/v HCl/1%v/v SDS cleaning hot solutions at 55 °C. Viability test after the treatment was done by auto-fluorescence % assay, with auto-fluorescence % expressed as the ratio of number of cells with red emitting chloroplasts, observed by confocal fluorescence microscopy, over the total number of cells observed in bright field. Measurements were repeated ten times for the statistical evaluation.

## 5.6 Rhodamine 123 blockage experiment

After the single PDA coating, experiments of incubation of coated diatoms with Rhodamine 123, were performed to test the effect of PDA on the dye incorporation in coated cells versus bare cells. 1  $\mu\text{L}$  of a Rhodamine 123 stock (10 mM) solution in DMSO was added to 0.99 mL of the culture medium, reaching a dye final concentration of 10  $\mu\text{M}$ . A confocal microscopy investigation was performed at different times of incubation, using fluorescein exc./em. parameters for Rhodamine123 detection, and TRITC exc./em. parameters for chloroplasts luminescence analysis.

## 5.7 PDA-assisted functionalization of living cells with Ag nanoparticles and SEM/EDX characterization

The diatoms cells, after PDA coating, were immersed and gently shaken in aqueous  $\text{AgNO}_3$  solution in distilled water (0.1 M aqueous solution, 2 mL). The reaction was performed for 24 h, to let silver NPs grow densely on the surface of biosilica. Then the structures were washed with deionized

water. After Ag NPs formation, external organic matter and eventually formed external Ag NPs were removed by successive washing cycles with deionized water and aqueous ethanol (10% EtOH, 90% H<sub>2</sub>O), until discoloration of the supernatant. Samples were casted directly on Si wafer and dried overnight under vacuum pump for SEM and EDX investigations.

**Acknowledgements** This work is supported by Fondo Sociale Europeo “Research for Innovation (REFIN)””; project no. 87429C9C—Algae vive per la bonifica dell’ambiente marino (AlgAmbiente). The research also refers to H2020-MSCA-ITN-2019 project 860125—BEEP (Bio-inspired and bionic materials for enhanced photosynthesis) and the EU project 800926-HyPhOE (Hybrid Electronics based on Photosynthetic Organisms).

**Author contribution** DV: experimental design, collection of biological resistance data, material characterization, writing paper; SRC, GMF, RR: experimental design and re-editing paper; CVG, GL: diatoms culture and coatings protocol, material characterization; MMG: AFM characterization; FP: confocal characterization; EA: SEM investigation.

## Declarations

**Conflict of interest** The authors have no conflicts to disclose.

**Consent to participate** All authors gave their consent to participate.

**Consent for publication** All authors gave their consent to publish.

**Ethics approval** Not applicable.

**Open Access** This article is licensed under a Creative Commons Attribution 4.0 International License, which permits use, sharing, adaptation, distribution and reproduction in any medium or format, as long as you give appropriate credit to the original author(s) and the source, provide a link to the Creative Commons licence, and indicate if changes were made. The images or other third party material in this article are included in the article’s Creative Commons licence, unless indicated otherwise in a credit line to the material. If material is not included in the article’s Creative Commons licence and your intended use is not permitted by statutory regulation or exceeds the permitted use, you will need to obtain permission directly from the copyright holder. To view a copy of this licence, visit <http://creativecommons.org/licenses/by/4.0/>.

## References

- Zheng, W., & Jiang, X. (2018). Synthesizing living tissues with microfluidics. *Accounts of Chemical Research*, 51(12), 3166–3173. <https://doi.org/10.1021/acs.accounts.8b00417>
- Custódio, C. A., & Mano, J. F. (2016). Cell surface engineering to control cellular interactions. *ChemNanoMat*, 2(5), 376–384. <https://doi.org/10.1002/cnma.201600047>
- Ariga, K., Fakhruddin, R., & Ariga, K. (2021). Nanoarchitectonics on living cells. *RSC Advances*, 11(31), 18898–18914. <https://doi.org/10.1039/d1ra03424c>
- Fakhruddin, R. F., Zamaleeva, A. I., Minullina, R. T., Konnova, S. A., & Paunov, V. N. (2012). Cyborg cells: Functionalisation of

- living cells with polymers and nanomaterials. *Chemical Society Reviews*, 41(11), 4189–4206. <https://doi.org/10.1039/c2cs15264a>
5. Lo Presti, M., Vona, D., Ragni, R., Cicco, S. R., & Farinola, G. M. (2021). Perspectives on applications of nanomaterials from shelled plankton. *MRS Communications*, 11(3), 213–225. <https://doi.org/10.1557/s43579-021-00032-0>
  6. Edalat, F., Sheu, I., Manoucheri, S., & Khademhosseini, A. (2012). Material strategies for creating artificial cell-instructive niches. *Current Opinion in Biotechnology*, 23(5), 820–825. <https://doi.org/10.1016/j.copbio.2012.05.007>
  7. Yang, S. H., Ko, E. H., Jung, Y. H., & Choi, I. S. (2011). Bioinspired functionalization of silica-encapsulated yeast cells. *Angewandte Chemie - International Edition*, 50(27), 6115–6118. <https://doi.org/10.1002/anie.201102030>
  8. Fakhruddin, R. F., & Minullina, R. T. (2009). Hybrid cellular-inorganic core-shell microparticles: Encapsulation of individual living cells in calcium carbonate microshells. *Langmuir*, 25(12), 6617–6621. <https://doi.org/10.1021/la901395z>
  9. Ko, E. H., Yoon, Y., Park, J. H., Yang, S. H., Hong, D., Lee, K. B., & Choi, I. S. (2013). Bioinspired, cytocompatible mineralization of silica-titania composites: Thermoprotective nanoshell formation for individual chlorella cells. *Angewandte Chemie - International Edition*, 52(47), 12279–12282. <https://doi.org/10.1002/anie.201305081>
  10. Krol, S., Nolte, M., Diaspro, A., Mazza, D., Magrassi, R., Gliozzi, A., & Fery, A. (2005). Encapsulated living cells on microstructured surfaces. *Langmuir*, 21(2), 705–709. <https://doi.org/10.1021/la047715q>
  11. Balkundi, S. S., Veerabadran, N. G., Matthew Eby, D., Johnson, G. R., & Lvov, Y. M. (2009). Encapsulation of bacterial spores in nanoorganized polyelectrolyte shells. *Langmuir*, 25(24), 14011–14016. <https://doi.org/10.1021/la900971h>
  12. Krol, S., Del Guerra, S., Grupillo, M., Diaspro, A., Gliozzi, A., & Marchetti, P. (2006). Multilayer nanoencapsulation. New approach for immune protection of human pancreatic islets. *Nano Letters*, 6(9), 1933–1939. <https://doi.org/10.1021/nl061049r>
  13. Hillberg, A. L., & Tabrizian, M. (2006). Biorecognition through layer-by-layer polyelectrolyte assembly: In-situ hybridization on living cells. *Biomacromolecules*, 7, 2742–2750.
  14. Yang, S. H., Kang, S. M., Lee, K. B., Chung, T. D., Lee, H., & Choi, I. S. (2011). Mussel-inspired encapsulation and functionalization of individual yeast cells. *Journal of the American Chemical Society*, 133(9), 2795–2797. <https://doi.org/10.1021/ja1100189>
  15. Wang, B., Wang, G., Zhao, B., Chen, J., Zhang, X., & Tang, R. (2014). Antigenically shielded universal red blood cells by polydopamine-based cell surface engineering. *Chemical Science*, 5(9), 3463–3468. <https://doi.org/10.1039/c4sc01120a>
  16. Zhou, Q., Liu, X., Tian, Y., Wu, M., & Niu, Z. (2017). Mussel-inspired polydopamine coating on tobacco mosaic virus: One-dimensional hybrid nanofibers for gold nanoparticle growth. *Langmuir*, 33(38), 9866–9872. <https://doi.org/10.1021/acs.langmuir.7b02252>
  17. Lee, H., Rho, J., & Messersmith, P. B. (2009). Facile conjugation of biomolecules onto surfaces via mussel adhesive protein inspired coatings. *Advanced Materials*, 21(4), 431–434. <https://doi.org/10.1002/adma.200801222>
  18. Zhang, X., Wang, S., Xu, L., Feng, L., Ji, Y., Tao, L., & Wei, Y. (2012). Biocompatible polydopamine fluorescent organic nanoparticles: Facile preparation and cell imaging. *Nanoscale*, 4(18), 5581–5584. <https://doi.org/10.1039/c2nr31281f>
  19. Ku, S. H., Ryu, J., Hong, S. K., Lee, H., & Park, C. B. (2010). General functionalization route for cell adhesion on non-wetting surfaces. *Biomaterials*, 31(9), 2535–2541. <https://doi.org/10.1016/j.biomaterials.2009.12.020>
  20. Hong, S., Kim, K. Y., Wook, H. J., Park, S. Y., Lee, K. D., Lee, D. Y., & Lee, H. (2011). Attenuation of the in vivo toxicity of biomaterials by polydopamine surface modification. *Nanomedicine*, 6(5), 793–801. <https://doi.org/10.2217/nmm.11.76>
  21. Ku, S. H., & Park, C. B. (2010). Human endothelial cell growth on mussel-inspired nanofiber scaffold for vascular tissue engineering. *Biomaterials*, 31(36), 9431–9437. <https://doi.org/10.1016/j.biomaterials.2010.08.071>
  22. Ambrico, M., Ambrico, P. F., Cardone, A., Della Vecchia, N. F., Ligonzo, T., Cicco, S. R., & D'Ischia, M. (2013). Engineering polydopamine films with tailored behaviour for next-generation eumelanin-related hybrid devices. *Journal of Materials Chemistry C*, 1(5), 1018–1028. <https://doi.org/10.1039/c2tc00480a>
  23. Cicco, S. R., Vona, D., Leone, G., De Giglio, E., Bonifacio, M. A., Cometa, S., & Farinola, G. M. (2019). In vivo functionalization of diatom biosilica with sodium alendronate as osteoactive material. *Materials Science and Engineering C*, 104(June), 109897. <https://doi.org/10.1016/j.msec.2019.109897>
  24. Cicco, S. R., Vona, D., De Giglio, E., Cometa, S., Mattioli-Belmonte, M., Palumbo, F., & Farinola, G. M. (2015). Chemically modified diatoms biosilica for bone cell growth with combined drug-delivery and antioxidant properties. *ChemPlusChem*, 80(7), 1104–1112. <https://doi.org/10.1002/cplu.201402398>
  25. Ragni, R., Scotognella, F., Vona, D., Moretti, L., Altamura, E., Ceccone, G., & Farinola, G. M. (2018). Hybrid photonic nanostructures by in vivo incorporation of an organic fluorophore into diatom algae. *Advanced Functional Materials*, 28(24), 1–9. <https://doi.org/10.1002/adfm.201706214>
  26. Vona, D., Ragni, R., Altamura, E., Albanese, P., Giangregorio, M. M., Cicco, S. R., & Farinola, G. M. (2021). Light-emitting biosilica by in vivo functionalization of phaeodactylum tricornerum diatom microalgae with organometallic complexes. *Applied Sciences (Switzerland)*. <https://doi.org/10.3390/app11083327>
  27. Della Rosa, G., Vona, D., Aloisi, A., Ragni, R., Di Corato, R., Lo Presti, M., & Rinaldi, R. (2019). Luminescent silica-based nanostructures from in vivo iridium-doped diatoms microalgae. *ACS Sustainable Chemistry and Engineering*, 7(2), 2207–2215. <https://doi.org/10.1021/acssuschemeng.8b04888>
  28. Leone, G., De la Cruz Valbuena, G., Cicco, S. R., Vona, D., Altamura, E., Ragni, R., & Farinola, G. M. (2021). Incorporating a molecular antenna in diatom microalgae cells enhances photosynthesis. *Scientific Reports*, 11(1), 1–12. <https://doi.org/10.1038/s41598-021-84690-z>
  29. Vona, D., Cicco, S. R., Ragni, R., Leone, G., Lo Presti, M., & Farinola, G. M. (2018). Biosilica/polydopamine/silver nanoparticles composites: New hybrid multifunctional heterostructures obtained by chemical modification of *Thalassiosira weissflogii* silica shells. *MRS Communications*, 8(3), 911–917. <https://doi.org/10.1557/mrc.2018.103>
  30. Grieco, C., Kohl, F. R., Hanes, A. T., & Kohler, B. (2020). Probing the heterogeneous structure of eumelanin using ultrafast vibrational fingerprinting. *Nature Communications*, 11(1), 1–9. <https://doi.org/10.1038/s41467-020-18393-w>
  31. Vona, D., Urbano, L., Bonifacio, M. A., De Giglio, E., Cometa, S., Mattioli-Belmonte, M., & Farinola, G. M. (2016). Data from two different culture conditions of *Thalassiosira weissflogii* diatom and from cleaning procedures for obtaining monodisperse nanostructured biosilica. *Data in Brief*, 8, 312–319. <https://doi.org/10.1016/j.dib.2016.05.033>
  32. Leone, G., Vona, D., De Giglio, E., Bonifacio, M. A., Cometa, S., Fiore, S., & Cicco, S. R. (2019). Data from in vivo functionalization of diatom mesoporous biosilica with bisphosphonates. *Data in Brief*, 24, 103831. <https://doi.org/10.1016/j.dib.2019.103831>
  33. Li, C. W., Chu, S., & Lee, M. (1989). Characterizing the silica deposition vesicle of diatoms. *Protoplasma*, 151(2–3), 158–163. <https://doi.org/10.1007/BF01403453>